

Premixed flame stability under shear-enhanced diffusion: Effect of the flow direction

Joel Daou * and Prabakaran Rajamanickam *Department of Mathematics, University of Manchester, Manchester, United Kingdom*

(Received 11 August 2023; accepted 28 November 2023; published 11 December 2023)

In the presence of shear-enhanced diffusion (Taylor dispersion), flame propagation is effectively anisotropic. This study focuses on the influence of the direction of a shear flow relative to the direction of propagation on the diffusional-thermal instabilities of premixed flames. The problem is addressed analytically using large activation energy asymptotics, complemented by numerical simulations, in the framework of a constant density two-dimensional model. The model, obtained by depth averaging of the governing equations in a Hele-Shaw configuration, accounts for shear-enhanced diffusion. A linear stability analysis is carried out analytically, leading to a dispersion relation involving three parameters: the Lewis number Le ; the Taylor-dispersion coefficient p , which is proportional to the Péclet number; and the angle ϕ between the direction of propagation of the unperturbed planar flame and the flow direction. Based on the dispersion relation, stability diagrams are determined in terms of the parameters, along with bifurcations curves identifying the nature of the instabilities observed. It is shown that cellular instabilities expected when $Le < 1$ can now occur as a result of Taylor dispersion in $Le > 1$ mixtures, provided the angle ϕ exceeds a critical value approximately equal to 75° . In general, it is found that an increase in ϕ from 0° to 90° has a stabilizing effect in subunity Lewis number mixtures $Le < 1$ and a destabilizing effect when $Le > 1$. Particular attention is devoted to the cellular long-wave instability encountered, which is found to be described by a modified Kuramoto-Sivashinsky equation. The equation involves the three aforementioned parameters and includes a dispersion term (a third-order spatial derivative) as well a drift term (first-order derivative) whenever $\phi \neq 0^\circ$ and $\phi \neq 90^\circ$, which is whenever the direction of the shear flow is neither parallel nor perpendicular to the direction of flame propagation.

DOI: [10.1103/PhysRevFluids.8.123202](https://doi.org/10.1103/PhysRevFluids.8.123202)

I. INTRODUCTION

The effect of shear-enhanced diffusion, or Taylor-Aris dispersion, on flame instabilities is a rich research topic whose investigation has only been recently initiated. Background and reports on related investigations can be found in [1–3] in the context of premixed combustion and in [4] in the case of nonpremixed combustion. These investigations have focused on flame stability in two special cases, for which the direction of the shear flow is either perpendicular [1,2] or parallel [3,4] to an initially planar flame whose stability is under investigation.

*joel.daou@manchester.ac.uk

Published by the American Physical Society under the terms of the [Creative Commons Attribution 4.0 International](https://creativecommons.org/licenses/by/4.0/) license. Further distribution of this work must maintain attribution to the author(s) and the published article's title, journal citation, and DOI.

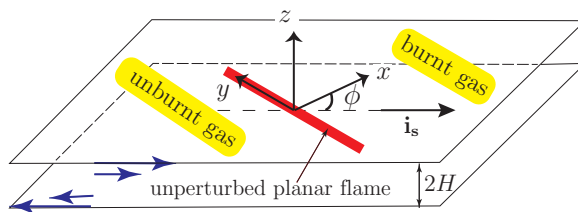


FIG. 1. Model configuration to investigate the diffusional-thermal instability of a planar flame propagating in a channel in a direction making an angle ϕ with the direction of a shear flow. A unit vector in the direction of the shear flow is $\mathbf{i}_s = c\mathbf{i} - s\mathbf{j}$, where $c = \cos \phi$, $s = \sin \phi$, and \mathbf{i} and \mathbf{j} are unit vectors in the x and y directions, respectively. In this study, ϕ is allowed to take arbitrary values in $[0^\circ, 90^\circ]$, with $\phi = 0^\circ$ and 90° corresponding to flame propagation in directions parallel and perpendicular to the flow direction, respectively

The present study is focused on premixed flames, and more specifically on the influence of the direction of a unidirectional shear flow on their well-known diffusional-thermal instabilities, allowing the direction to be arbitrary with respect to the flame. The main motivation for our focus is that thick flames propagating in shear flows, occurring, say, in narrow channels, are subject to diffusion enhancement by Taylor dispersion as described in recent publications [5–7]. Since the enhancement of diffusion occurs in the flow direction, and not in a transverse direction, this leads to problems involving anisotropic diffusion. As a consequence of this anisotropy, the direction of the flow with respect to the flame becomes a crucial factor when studying flame stability. The present investigation is dedicated to elucidating the role such factor plays. Our goal is best achieved by considering flame propagation and stability when the direction of propagation is arbitrary with respect to that of the shear flow. Since our main concern is the coupling between Taylor dispersion and the thermodiffusive flame instabilities [8,9], we adopt a simple model based on the thermodiffusive approximation of constant density and constant transport properties.

As a convenient configuration for the investigation, we adopt a Hele-Shaw burner configuration similar to that adopted in a variety of notable experimental and theoretical studies on flame instabilities, such as [10–16]. An important additional aspect included in our configuration, however, is the presence of a unidirectional shear flow. Specifically, we consider an idealized model corresponding to flame propagation between two closely spaced parallel plates moving in opposite directions so as to generate a shear Couette flow (with zero mean) of the reactive gas between them, as sketched in Fig. 1. The plates are assumed to be adiabatic, and the direction of the shear flow is taken to be arbitrary with respect to that of the initially planar unperturbed flame whose stability is being investigated. The findings should therefore complement significantly those of [1–4], which did not consider the effect of varying the angle ϕ , which is important in order to quantify the effect of Taylor-dispersion-induced anisotropic diffusion on flame propagation and stability.

The paper is structured as follows. The model formulation is given in Sec. II within a Hele-Shaw configuration involving a shear flow and includes two-dimensional depth-averaged governing equations which explicitly account for Taylor dispersion and the angle ϕ . The problem is examined analytically in Secs. III–VI, using large activation energy asymptotics. A formula for the propagation speed of the planar flame with arbitrary Lewis number and arbitrary direction of propagation is derived in Sec. III. This is followed in Sec. IV by a reformulation of the problem for nearly equidiffusional flames suitable for the linear stability analysis carried out in Sec. V. The stability analysis leads to an explicit dispersion relation whose implications are examined in detail in Sec. VI. The results include the determination of the stability and instability regions in the parameter space, the characterization of the nature of the bifurcations involved, and the derivation of a modified Kuramoto-Sivashinsky equation which explicitly accounts for Taylor dispersion, the angle ϕ , and the Lewis number. The analytical findings are complemented by two-dimensional

numerical computations for selected illustrative cases reported in Sec. VII. A summary of the main findings and conclusions are provided in Sec. VIII.

II. MODEL

We begin by formulating the problem in a frame attached to the unperturbed planar flame front shown in Fig. 1. The governing equations are two dimensional as they are obtained upon depth averaging in the z direction, as done in [1], which may be consulted for details and background. The equations are written in terms of the coordinates x and y , whose axes are as shown in the figure, with the x axis making an angle ϕ with respect to the direction of the shear flow (assumed to be a Couette flow with zero mean). Using the abbreviations $c = \cos \phi$ and $s = \sin \phi$, the nondimensional problem is given by

$$\frac{\partial \theta}{\partial t} + U \frac{\partial \theta}{\partial x} = (1 + p^2 c^2) \frac{\partial^2 \theta}{\partial x^2} + (1 + p^2 s^2) \frac{\partial^2 \theta}{\partial y^2} - 2p^2 cs \frac{\partial^2 \theta}{\partial x \partial y} + \omega, \quad (1a)$$

$$\frac{\partial y_F}{\partial t} + U \frac{\partial y_F}{\partial x} = \frac{1}{\text{Le}} (1 + p^2 c^2 \text{Le}^2) \frac{\partial^2 y_F}{\partial x^2} + \frac{1}{\text{Le}} (1 + p^2 s^2 \text{Le}^2) \frac{\partial^2 y_F}{\partial y^2} - 2p^2 cs \text{Le} \frac{\partial^2 y_F}{\partial x \partial y} - \omega, \quad (1b)$$

$$\theta = 0, \quad y_F = 1 \quad \text{as } x \rightarrow -\infty, \quad (1c)$$

$$\theta_x = 0, \quad y_F = 0 \quad \text{as } x \rightarrow +\infty \quad (1d)$$

in terms of the scaled mass fraction of the fuel y_F and the nondimensional temperature θ . Here U is the nondimensional propagation speed of the unperturbed front with respect to the gas and ω is the reaction rate given by

$$\omega = \frac{\beta^2}{2\text{Le}} y_F \exp\left(\frac{\beta(\theta - 1)}{1 + \alpha_h(\theta - 1)}\right),$$

involving the Zel'dovich number β , which is assumed to be large, and the heat-release parameter $\alpha_h \approx 0.85$. An important parameter appearing in the equations is the Taylor-dispersion coefficient $p^2 \equiv \gamma \text{Pe}^2$, where Pe is the Péclet number and γ a numerical coefficient determined by the flow profile [1]. For a Couette flow $\gamma = \frac{1}{20}$ when the Péclet number is based on the maximum flow amplitude and the channel half-width H . Another important parameter is of course the Lewis number Le . For nondimensionalization, we have chosen S_L as unit speed, δ_L as unit length, and δ_L/S_L as unit time, with S_L and δ_L the laminar flame speed and its thickness (for $\beta \gg 1$) in the absence of Taylor dispersion.

It is worth noting that Eqs. (1a) and (1b) imply the existence of two effective Lewis numbers in the x and y directions given by

$$\text{Le}_x = \frac{(1 + p^2 c^2) \text{Le}}{1 + p^2 c^2 \text{Le}^2}, \quad \text{Le}_y = \frac{(1 + p^2 s^2) \text{Le}}{1 + p^2 s^2 \text{Le}^2}. \quad (2)$$

In the absence of shear flow $p = 0$, $\text{Le}_x = \text{Le}_y = \text{Le}$, that is to say, the effective Lewis numbers are the same as the molecular Lewis number Le . However, when $p \neq 0$, Le_x , Le_y , and Le assume in general distinct values. In particular, when $p \gg 1$,

$$\text{Le}_x = \frac{1}{\text{Le}}, \quad \text{Le}_y = \text{Le} \quad \text{for longitudinal propagation } (c = 1, s = 0),$$

$$\text{Le}_x = \text{Le}, \quad \text{Le}_y = \frac{1}{\text{Le}} \quad \text{for transverse propagation } (c = 0, s = 1).$$

The fact that the effective Lewis numbers can assume values quite distinct from Le , in particular its inverse value $1/\text{Le}$, in the presence of Taylor dispersion, will have profound implications on the diffusive-thermal flame instability, as will be confirmed below.

III. THE PLANAR FLAME FOR ARBITRARY LEWIS NUMBER AND DIRECTION OF PROPAGATION

The problem (1a)–(1d) admits one-dimensional stationary solutions independent of t and y , which correspond to planar flames propagating with respect to the unburnt mixture with speed U . The propagation speed U and the corresponding solutions are determined from the one-dimensional eigen-boundary-value problem

$$U \frac{d\theta}{dx} = (1 + p^2 c^2) \frac{d^2\theta}{dx^2} + \omega, \quad (3a)$$

$$U \frac{dy_F}{dx} = \frac{1}{\text{Le}} (1 + p^2 c^2 \text{Le}^2) \frac{d^2 y_F}{dx^2} - \omega, \quad (3b)$$

$$\theta = 0, \quad y_F = 1 \quad \text{as } x \rightarrow -\infty, \quad (3c)$$

$$\theta = 1, \quad y_F = 0 \quad \text{as } x \rightarrow +\infty \quad (3d)$$

The solution is given in the limit $\beta \rightarrow \infty$ by

$$\theta = \begin{cases} \exp\left(\frac{Ux}{1+p^2c^2}\right) & y_F = \begin{cases} 1 - \exp\left(\frac{\text{Le}Ux}{1+p^2c^2\text{Le}^2}\right) & \text{for } x < 0 \\ 0 & \text{for } x > 0, \end{cases} \end{cases} \quad (4)$$

with

$$U = \frac{1 + p^2 c^2}{(1 + p^2 c^2 \text{Le}^2)^{1/2}}. \quad (5)$$

A simple way to obtain these formulas is to note first that the problem reduces, when $pc = 0$, to a classical problem whose solution is given by (4) and (5) with pc set to zero, which implies in particular that $U = 1$. Next it can be checked that this classical problem is also recovered in the general case with arbitrary values of pc if the problem (3) is written in terms of the primed quantities

$$x' = \frac{x}{(1 + p^2 c^2 \text{Le}^2)^{1/2}}, \quad U' = \frac{(1 + p^2 c^2 \text{Le}^2)^{1/2} U}{1 + p^2 c^2}, \quad \text{Le}' = \frac{(1 + p^2) \text{Le}}{1 + p^2 c^2 \text{Le}^2}.$$

The solution in terms of the primed quantities is thus the classical one, in particular $U' = 1$; returning to the nonprimed quantities, we have the solution given by (4) and (5).

IV. PROBLEM FORMULATION IN THE NEAR-EQUIDIFFUSIONAL FLAME APPROXIMATION

The analysis of the stability of the planar flame (depicted in Fig. 1) is most consistently carried out analytically in the limit $\beta \rightarrow \infty$ using the so-called near-equidiffusional flame approximation based on the assumption that the Lewis number deviates little from unity. Within this approximation, the reduced Lewis number $l \equiv \beta(\text{Le} - 1)$ is $O(1)$ and Eqs. (1a) and (1b) can be written in terms of the leading-order temperature $\theta^0 \sim \theta$ and $h \sim \beta(\theta + y_F - 1)$. The reformulated problem is given by the equations

$$\theta_t^0 + U \theta_x^0 = (1 + p^2 c^2) \theta_{xx}^0 + (1 + p^2 s^2) \theta_{yy}^0 - 2p^2 c s \theta_{xy}^0, \quad (6)$$

$$\begin{aligned} h_t + U h_x &= (1 + p^2 c^2) h_{xx} + (1 + p^2 s^2) h_{yy} - 2p^2 c s h_{xy} \\ &+ l[(1 - p^2 c^2) \theta_{xx}^0 + (1 - p^2 s^2) \theta_{yy}^0 + 2p^2 c s \theta_{xy}^0], \end{aligned} \quad (7)$$

which are applicable outside an infinitely thin reaction sheet, given by, say, $x = f(y, t)$, subject to the boundary conditions

$$\theta^0 = 0, \quad h = 0 \quad \text{as } x \rightarrow -\infty, \quad (8)$$

$$\theta^0 = 1, \quad h \text{ has no exponential growth} \quad \text{as } x \rightarrow +\infty \quad (9)$$

and the jump conditions

$$[[\theta^0]] = 0, \quad [[h]] = 0, \quad (10a)$$

$$[[h_x]] + \frac{1 + f_y^2 - p^2(c + sf_y)^2}{1 + f_y^2 + p^2(c + sf_y)^2} l [[\theta_x^0]] = 0, \quad (10b)$$

$$[1 + f_y^2 + p^2(c + sf_y)^2]^{1/2} [[\theta_x^0]] = -\exp\left(\frac{h}{2}\right) \quad (10c)$$

applicable at $x = f(y, t)$. Here we have used the notation $[[\psi]] = \psi(x = f^+) - \psi(x = f^-)$. The reader is referred to [1] for a justification of the near-equidiffusional flame reformulation of the problem incorporating Taylor dispersion, used herein with coordinates suitable for a rotated frame, and to Appendix A for a justification of the jump conditions (10).

V. LINEAR STABILITY ANALYSIS

The planar flame solution (denoted by an overbar) whose stability is being investigated is governed by Eqs. (6)–(10) with $\partial/\partial t = 0$ and $\partial/\partial y = 0$. The solution is

$$\bar{f} = 0, \quad \bar{\theta} = \begin{cases} \exp\left(\frac{Ux}{1+p^2c^2}\right) & \bar{h} = \begin{cases} -\frac{l(1-p^2c^2)Ux}{(1+p^2c^2)^2} \exp\left(\frac{Ux}{1+p^2c^2}\right) & \text{for } x < 0 \\ 0 & \text{for } x > 0, \end{cases} \end{cases} \quad (11)$$

where the propagation speed U is given by

$$U = (1 + p^2c^2)^{1/2}. \quad (12)$$

A normal-mode stability analysis can now be applied to the basic solution (11) by considering perturbations of the form

$$\begin{bmatrix} f \\ \theta^0 \\ h \end{bmatrix} = \begin{bmatrix} \bar{f} \\ \bar{\theta}(x) \\ \bar{h}(x) \end{bmatrix} + \delta e^{\sigma t + iky} \begin{bmatrix} \hat{f} \\ \hat{\theta}(x) \\ \hat{h}(x) \end{bmatrix}, \quad (13)$$

where δ is a small number representing the amplitude of the perturbation and k and σ are a real and a complex numbers representing its wavelength and its growth rate, respectively. The stability analysis leads, as shown in Appendix B, to a dispersion relation which is most conveniently expressed in terms of the variables

$$\tilde{\sigma} = \sigma + ig\tilde{k}, \quad \tilde{k}^2 = k^2 \frac{1 + p^2}{1 + p^2c^2}, \quad g = \frac{p^2cs}{\sqrt{1 + p^2}}. \quad (14)$$

The dispersion relation reads

$$2\Gamma^2(\Gamma - 1) + \frac{l}{1 + p^2c^2} \left((\Gamma - 2\tilde{\sigma} - 1)(1 - p^2c^2) + 4ig\tilde{k}(\Gamma - 1) - \frac{4p^2\tilde{k}^2}{1 + p^2} [1 - c^2(p^2 + 2)] \right) = 0, \quad (15)$$

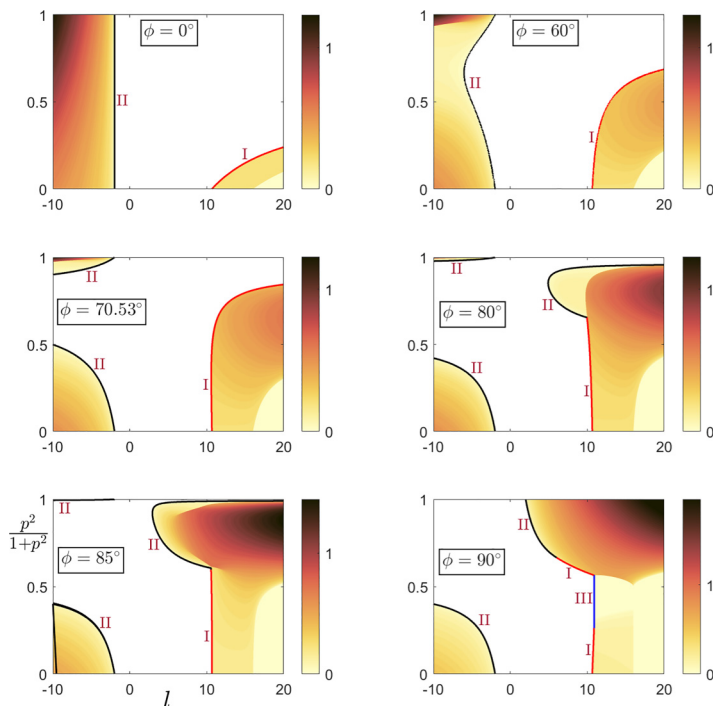


FIG. 2. Bifurcation curves and stability and instability regions in the l - p [or more precisely l versus $p^2/(1+p^2)$] plane for selected values of the angle ϕ . Colored regions correspond to unstable flames and white regions to stable ones. The color scale measures the magnitude of the scaled wave number \tilde{k} corresponding to the most unstable mode. The case $\phi = 0^\circ$ corresponds to longitudinal flame propagation (i.e., propagation parallel to the shear flow) and the case $\phi = 90^\circ$ to transverse propagation. The labels I, II, and III on the curves refer to the type of bifurcation following the terminology of [17], as explained in the text and in Fig. 5.

where $\Gamma = \sqrt{1 + 4\tilde{\sigma} + 4\tilde{k}^2}$. We note that the dispersion relation (15) reduces to that derived by Sivashinsky [8] when $p = 0$ and to that derived by Daou [1] in the case of longitudinal propagation corresponding to $\phi = 0^\circ$.

VI. IMPLICATIONS OF THE DISPERSION RELATION

A. Instability domains and bifurcation curves

For given values of l , p , and ϕ , we can solve numerically Eq. (15) for $\tilde{\sigma}(\tilde{k})$ or $\sigma(k)$ (with $c = \cos \phi$ and $s = \sin \phi$), with instability being implied when $\text{Re}(\sigma)$ is positive. An extensive set of results is thus obtained and is summarized in Figs. 2–4. For selected values of the angle ϕ , bifurcation curves and stability and instability regions are determined in the l - p plane in Fig. 2 and in the l - k plane in Fig. 3. Similarly, in Fig. 4 the stability and instability regions are determined in the ϕ - p plane. Strictly speaking, in Figs. 2 and 4 we use instead of p the equivalent parameter $p^2/(1+p^2)$, which increases monotonically from zero to one as p increases from zero to infinitely large values. Furthermore, in these two figures we have labeled the bifurcation curves, separating the stable and unstable regions, by roman numerals I, II, and III. These numerals refer to type-I, -II, and -III bifurcations, respectively, following the terminology used in [17,18]. A type-I bifurcation characterizes a finite-wavelength instability whose onset occurs at $k = k_c \neq 0$, while type-II and -III bifurcations characterize long-wave instabilities whose onset corresponds to $k = 0$. These three types are schematically illustrated in Fig. 5, where a brief explanation is provided in the caption.

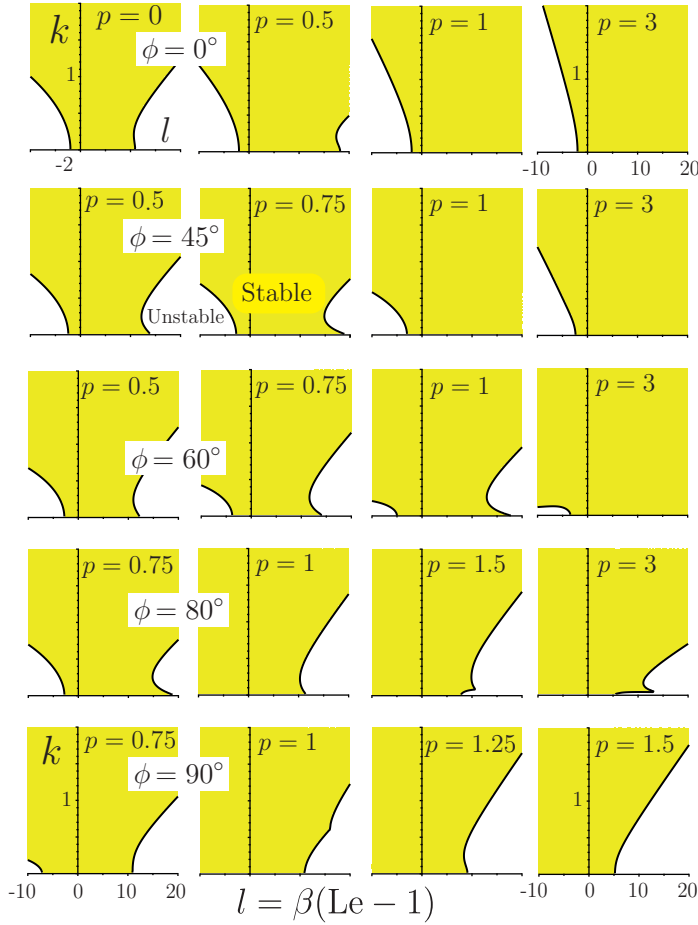


FIG. 3. Bifurcation curves and stability and instability regions in the l - k plane for selected values of the angle ϕ and p . Here the shaded regions are stable.

Figures 2–4 demonstrate the significant combined influence of the Taylor-dispersion coefficient p and the angle ϕ on the stability regions and identify the nature of the instability in the parameter space. Several important conclusions can be inferred from the figures.

(i) In subunity Lewis-number mixtures, $Le < 1$ or $l < 0$, and in the presence of Taylor dispersion, $p \neq 0$, an increase of ϕ from 0° to 90° has a stabilizing effect on the cellular (long-wave type-II) instability. This is seen, e.g., from the increase of the size of the white stable region in the negative- l side of Fig. 2 and the top and middle rows in Fig. 4.

(ii) In mixtures with $Le > 1$ or $l > 0$, a cellular instability can emerge for p above a critical value, if the angle ϕ is greater than approximately 75° (see analysis below). In general, an increase in ϕ from 0° to 90° has a destabilizing effect, in contrast to the previous case corresponding to $l < 0$.

(iii) A point worth emphasizing is that the long-wave type-II instability, which is the classical cellular instability encountered in subunity Lewis number mixtures and described by the celebrated Kuramoto-Sivashinsky equation [19], is predicted now for both $l < 0$ and $l > 0$, provided p and ϕ are chosen appropriately. Specifically, this instability is expected to occur as we cross the type-II bifurcation curves identified in the figures, where the color scale indicates that $k = 0$ in the close vicinity of these curves. In the following, we will focus on this long-wave type-II instability, which leads to a modified Kuramoto-Sivashinsky equation, to be derived next.

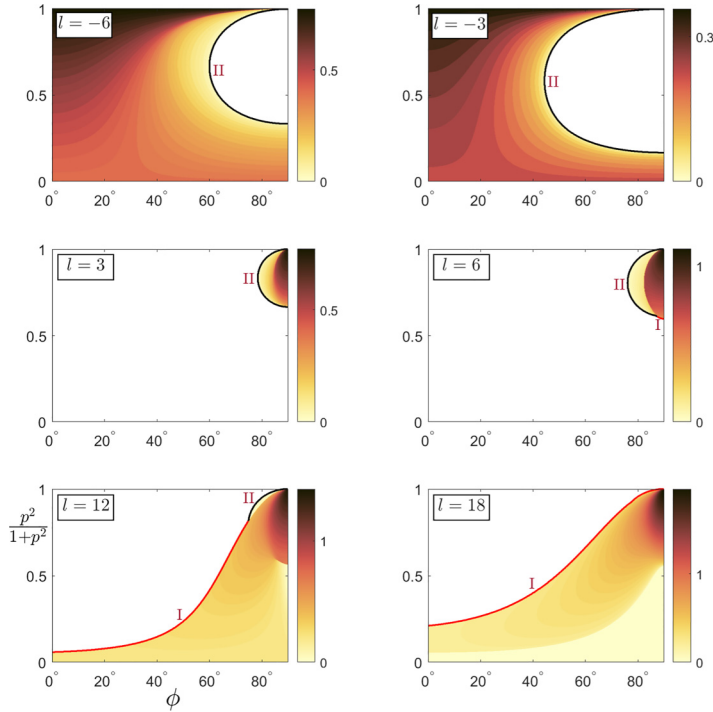


FIG. 4. Bifurcation curves and stability and instability regions in the ϕ - p [or more precisely ϕ versus $p^2/(1+p^2)$] plane for selected values of the reduced Lewis number l . Colored regions correspond to unstable flames and white regions to stable ones. The color scale measures the magnitude of the scaled wave number \tilde{k} corresponding to the most unstable mode. The labels I, II, and III on the curves refer to the type of bifurcation following the terminology of [17], as explained in the text and in Fig. 5.

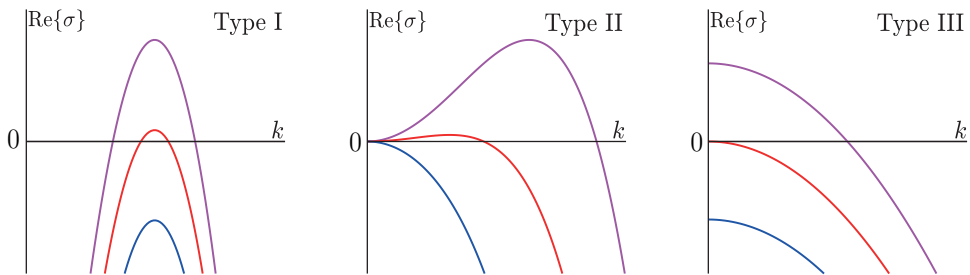


FIG. 5. Schematic illustration of the three types of bifurcation identified in Figs. 2 and 4, following the terminology of [17]. Plotted is the growth rate $\text{Re}(\sigma)$ as a function of the wave number k near the instability onset occurring at, say, $k = k_c$. The curves move up as we cross from stable to unstable regions in the parameter space. Type I is a finite-wavelength instability corresponding to $k_c \neq 0$, while types II and III are long-wave instabilities with $k_c = 0$. Note that in a type-II bifurcation $\text{Re}(\sigma)(k = 0)$ remains equal to zero, while in a type-III bifurcation $\text{Re}(\sigma)(k = 0)$ changes sign from negative to positive as we cross from stable to unstable regions in the parameter space. Mathematically, a type-II bifurcation requires the three conditions $\text{Re}(\sigma) = 0$, $d\text{Re}(\sigma)/dk = 0$, and $d^2\text{Re}(\sigma)/dk^2 = 0$ to be met at $k = 0$, as shown in the figure. Only the first two of these conditions are required for type-I and type-III bifurcations to be satisfied at $k = k_c \neq 0$ and $k = 0$, respectively, where $d^2\text{Re}(\sigma)/dk^2 < 0$.

B. Long-wave instability and the modified Kuramoto-Sivashinsky equation

1. Derivation of an evolution equation in the weakly nonlinear regime

Note that the dispersion relation (15) has always one root $\tilde{\sigma}(\tilde{k})$ such that $\tilde{\sigma}(0) = 0$. It is the presence of this root that is at the origin of the long-wave (type-II) instability under consideration. The onset of this instability is determined by the condition $d^2\tilde{\sigma}/d\tilde{k}^2|_{\tilde{k}=0} = 0$, which specifies the critical values l_c ,

$$l_c = \frac{-2(1+p^2)(1+p^2c^2)}{1+(3c^2-1)p^2+p^4c^2}, \quad (16)$$

for the reduced Lewis number l . In the neighborhood of $l = l_c$, the growth rate $\tilde{\sigma}$ can be expanded in a Taylor series as

$$\tilde{\sigma} = \frac{l-l_c}{l_c}\tilde{k}^2 - \frac{2igl_c}{1+p^2c^2}\tilde{k}^3 - a\tilde{k}^4 + \dots, \quad (17)$$

where

$$a = 3 - \frac{l_c(1-p^2c^2)}{2(1+p^2c^2)} + \frac{4g^2l_c^2}{(1+p^2c^2)^2}.$$

Since $\tilde{\sigma} = \sigma + ig\tilde{k}$, it then follows using (14) that

$$\sigma = -ig\alpha k + \frac{l-l_c}{l_c}\alpha^2 k^2 - \frac{2igl_c}{1+p^2c^2}\alpha^3 k^3 - a\alpha^4 k^4 + \dots, \quad (18)$$

where

$$\alpha = \frac{(1+p^2)^{1/2}}{(1+p^2c^2)^{1/2}}. \quad (19)$$

This expansion allows us to readily write down the linear part of a Kuramoto-Sivashinsky (KS) type of equation suitable to describe the instability near onset. The ik and ik^3 terms in this expansion indicate the additional presence of a first-order spatial derivative f_y (drift) and a third-order spatial derivative f_{yyy} (dispersion) in such a modified KS equation. The full modified KS equation includes in fact a nonlinear term which is needed to saturate the instability near onset. The nonlinear term can be derived using a semiheuristic kinematic argument as explained in [19] and as done below. The resulting full equation reads

$$f_t + \alpha_1 f_y + \alpha_2 f_{yy} + \alpha_3 f_{yyy} + \alpha_4 f_{yyyy} + \alpha' f_y^2 = 0, \quad (20)$$

where the coefficients are given by

$$\alpha_1 = g\alpha \equiv \frac{p^2cs}{(1+p^2c^2)^{1/2}}, \quad (21a)$$

$$\alpha_2 = \frac{l-l_c}{l_c}\alpha^2, \quad (21b)$$

$$\alpha_3 = -\frac{2gl_c}{1+p^2c^2}\alpha^3, \quad (21c)$$

$$\alpha_4 = \left(3 - \frac{l_c(1-p^2c^2)}{2(1+p^2c^2)} + \frac{4g^2l_c^2}{(1+p^2c^2)^2}\right)\alpha^4, \quad (21d)$$

$$\alpha' = \frac{1+p^2}{2(1+p^2c^2)^{3/2}}, \quad (21e)$$

with l_c and α being as given in (16) and (19).

The coefficients α_1 , α_2 , α_3 , and α_4 of the linear terms in (20) are obtained directly from the expansion (18) of the dispersion relation, as mentioned above, since the linear part of (20) is equivalent to (18) in the case of normal modes $f(y, t) \propto e^{\sigma t + iky}$. As for the coefficient α' of the nonlinear term, this can be determined by a simple analysis as follows. We start from the eikonal equation (10) given in Appendix A, namely,

$$F_t + \mathbf{v} \cdot \nabla F = S_L(\mathbf{n})|\nabla F|. \quad (22)$$

In this equation, the flame front is described by the relation $F(\mathbf{x}, t) = x - f(y, t) = 0$, \mathbf{v} is the flow velocity, and $S_L(\mathbf{n})$ is the local burning speed of a quasiplanar front which depends on the local normal unit vector $\mathbf{n} = \nabla F/|\nabla F| = (\mathbf{i} - f_y \mathbf{j})/(1 + f_y^2)^{1/2}$. According to (A7) we have

$$S_L(\mathbf{n}) = [1 + p^2(\mathbf{n} \cdot \mathbf{i}_s)^2]^{1/2}. \quad (23)$$

Also, since the frame of reference has been chosen to be attached to the unperturbed flame which is moving with respect to the gas with speed $-U\mathbf{i}$, the flow velocity in this frame is $\mathbf{v} = U\mathbf{i}$, where $U = (1 + p^2c^2)^{1/2}$ according to (12). It follows that (22) may be written as $-f_t + U = S_L(\mathbf{n})(1 + f_y^2)^{1/2}$, whence

$$\begin{aligned} f_t &= (1 + p^2c^2)^{1/2} - [1 + p^2(\mathbf{n} \cdot \mathbf{i}_s)^2]^{1/2}(1 + f_y^2)^{1/2} \\ &= (1 + p^2c^2)^{1/2} - \left(1 + p^2 \frac{(c + sf_y)^2}{1 + f_y^2}\right)^{1/2} (1 + f_y^2)^{1/2}. \end{aligned}$$

A Taylor expansion of the right-hand side of the preceding equation for small values of f_y implies that

$$f_t = -\alpha_1 f_y - \alpha' f_y^2 + \dots,$$

where the coefficient α' of the nonlinear term and also the coefficient α_1 of f_y are as given in (21), which completes the derivation.

2. Comments on the modified Kuramoto-Sivashinsky equation

We close this section by noting that Eq. (20) reduces to the equation derived by Sivashinsky, namely,

$$f_t - \left(1 + \frac{l}{2}\right)f_{yy} + 4f_{yyyy} + \frac{1}{2}f_y^2 = 0$$

when $p = 0$, as it should. When $\phi = 0^\circ$ and 90° , it reduces, respectively, to

$$\begin{aligned} f_t - \left(1 + \frac{l}{2}\right)f_{yy} + \frac{4 + 2p^2}{1 + p^2}f_{yyyy} + \frac{1}{2(1 + p^2)^{1/2}}f_y^2 &= 0, \\ f_t - \left(1 + \frac{l(1 - p^2)}{2(1 + p^2)}\right)(1 + p^2)f_{yy} + \frac{4 - 2p^2}{1 - p^2}(1 + p^2)^2f_{yyyy} + \frac{1}{2}(1 + p^2)f_y^2 &= 0. \end{aligned}$$

Note that the coefficients α_1 and α_3 of the odd space derivatives in (20) include the coefficient g , which is proportional to $p^2cs = p^2 \cos \phi \sin \phi$. Therefore, the first-order derivative f_y term (representing convection along the front associated with cross diffusion) and the third-order derivative f_{yyy} (dispersive term) only exist when the condition $p^2 \cos \phi \sin \phi \neq 0$ is satisfied; this requires the presence of Taylor dispersion, $p \neq 0$, and the planar flame to be in a direction which is neither parallel nor perpendicular to that of the shear flow, $\phi \neq 0^\circ$ and $\phi \neq 90^\circ$.

For weakly unstable flames, a rescaling of y , t , and f in Eq. (20) leads to the simplified form

$$f_t + \delta_1 f_y + f_{yy} + \delta_3 f_{yyy} + f_{yyyy} + \frac{1}{2}f_y^2 = 0, \quad (24)$$

involving two free parameters δ_1 and δ_3 given by

$$\delta_1 = \frac{\alpha_1}{\alpha_2^2} \sqrt{\alpha_2 \alpha_4}, \quad \delta_3 = \frac{\alpha_3}{\sqrt{\alpha_2 \alpha_4}}.$$

We note that equations similar to (24), including the third-order derivative dispersive term, have been found in a variety of studies in the literature, although not in combustion. Such equations are often referred to as dispersive (or dispersively modified) KS equations; see, e.g., [20–22] and references therein. These and related publications have mainly focused on assessing the effect of the dispersive term on the overall dynamics which is, as in the case of the classical KS equation, quite rich and comprises a variety of solutions including chaotic ones. In general, it is found that the dispersive term typically leads to regularization (or laminarization) of the solutions if the magnitude of its coefficient is large enough [20,21]. In this paper we do not pursue a mathematical or computational investigation of the solutions to Eq. (24). Suffice it to note that the coefficient δ_3 of the dispersive term in this equation may take both positive and negative values, as its sign is opposite to that of the critical reduced Lewis number l_c given by (16). This implies that the dynamics of weakly unstable flames is expected to be affected differently by the dispersive term, depending on whether the mixture Lewis number is greater or less than unity.

C. Long-wave instability domain based on the Kuramoto-Sivashinsky equation

The long-wave instability addressed in the preceding section corresponds to the coefficient of f_{yy} in (20) being positive, that is, to the inequality $\alpha_2(l, p, \phi) > 0$, where α_2 is given by (21b). For this to be the case, it is necessary however that the coefficient α_4 given by (21d) remains positive,¹ which leads to a well-posed problem. The regions of stability and instability can thus be determined in the l - p - ϕ parameter space. Representative results are shown in Fig. 6, where the stability and instability regions are depicted in the l - p plane for selected values of the angle ϕ . The figure shows that for $-2 < l < 2$ the long-wave instability does not occur, while for any other value of l , positive or negative, the instability occurs provided ϕ and p are appropriately chosen. The blue asymptotes in the figure correspond to $p = p_1$ and $p = p_2$, where p_1 and p_2 are positive real numbers such that

$$p_1^2 = \frac{1 - 3c^2 - \sqrt{(9c^2 - 1)(c^2 - 1)}}{2c^2}, \quad p_2^2 = \frac{1 - 3c^2 + \sqrt{(9c^2 - 1)(c^2 - 1)}}{2c^2}. \quad (25)$$

Since the argument of the square root in these expressions is negative for $c^2 > \frac{1}{9}$, these asymptotes only exist when $c \leq \frac{1}{3}$, that is, when the angle ϕ is in the range

$$90^\circ > \phi > \arccos\left(\frac{1}{3}\right) \approx 70.53^\circ. \quad (26)$$

The asymptotes are important in defining the long-wave instability domain in terms of the parameters. Specifically, when $\phi < 70.53^\circ$ the long-wave instability can only occur in subunity Lewis mixtures $l < 0$, whatever the value of p . In contrast, when $\phi > 70.53^\circ$, the long-wave instability can occur in mixtures with $l > 0$ for values of p exceeding p_1 but less than p_2 , as well as in mixtures with $l < 0$ for $p < p_1$ and $p > p_2$; see e.g. the case $\phi = 85^\circ$ in Fig. 6. In all cases, as mentioned above, a necessary condition for the occurrence of the long-wave instability predicted by Eq. (20) is that $\alpha_4 > 0$, and this turns out to be the case, except in a small region in the ϕ - p plane which is bounded by the rectangular domain $[85.35^\circ, 90^\circ] \times [1, \sqrt{2}]$. This small region where $\alpha_4 < 0$ is shown colored in yellow in Fig. 7, along with the asymptotic values p_1 and p_2 given by (25) and plotted as solid lines. According to the theoretical analysis of this section based on the KS equation (20), the long-wave instability is predicted to occur in $l > 0$ mixtures for values of ϕ and p

¹Note that a negative value of α_4 would contradict the requirement for a type-II bifurcation to have the critical wavenumber k_c equal to zero at the onset of instability corresponding to $\alpha_2 = 0$.

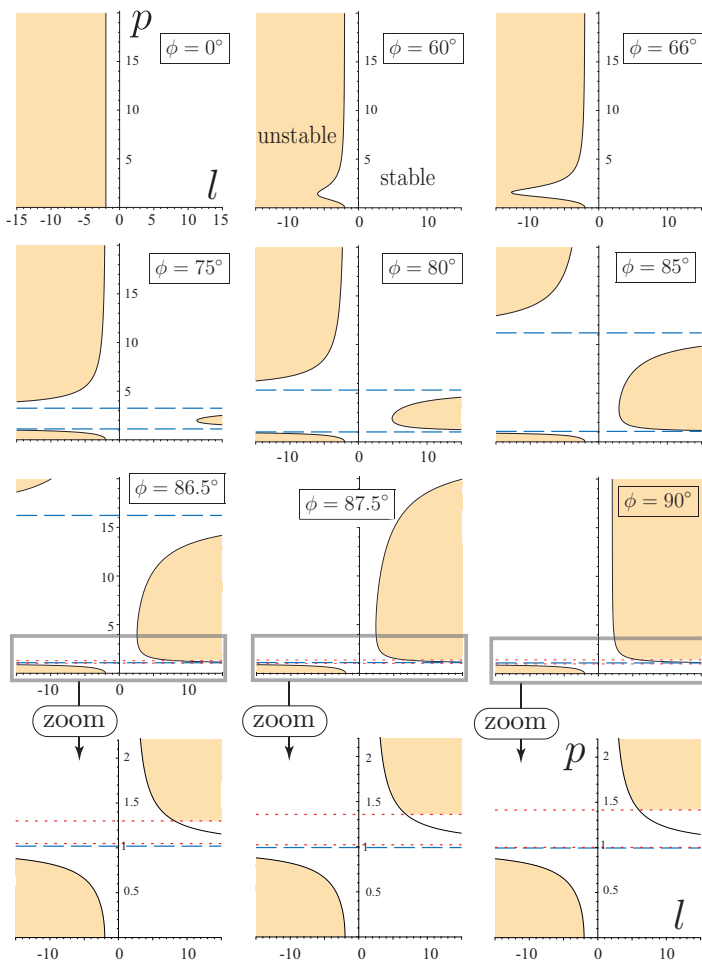


FIG. 6. Bifurcation curves and stability and instability regions in the l - p plane [based on the KS equation (20)] for selected values of the angle ϕ . The shaded regions are unstable. The blue dashed lines represent the asymptotes $p = p_1$ and $p = p_2$ specified by (25) which appear when $\phi > \arccos(\frac{1}{3}) \approx 70.53^\circ$. The red dotted lines delimit the region where $\alpha_4 < 0$, and therefore the KS equation (20) is not applicable; these appear when $\phi > 85.35^\circ$.

to the right of the blue C-shaped solid curve excluding the yellow region. In actuality, the long-wave instability under consideration is overshadowed by other instabilities for values of ϕ and p lying in the region between the solid C-shaped curve and the dashed C-shaped curve. The latter is based on numerical calculations accounting for all roots of the dispersion relation, rather than the root leading to the long-wave instability described by Eq. (20). Therefore, the actual region for the occurrence of the long-wave instability in $l > 0$ mixtures is to the right of the dashed C-shaped curve excluding the yellow region, which requires in particular the angle ϕ to exceed approximately 75° [instead of the value 70.53 prescribed by (26)].

VII. NUMERICAL SIMULATIONS

In this section we present time-dependent simulations in order to illustrate the theoretical findings, focusing mainly on the long-wave (type-II) instability and confirming in particular its

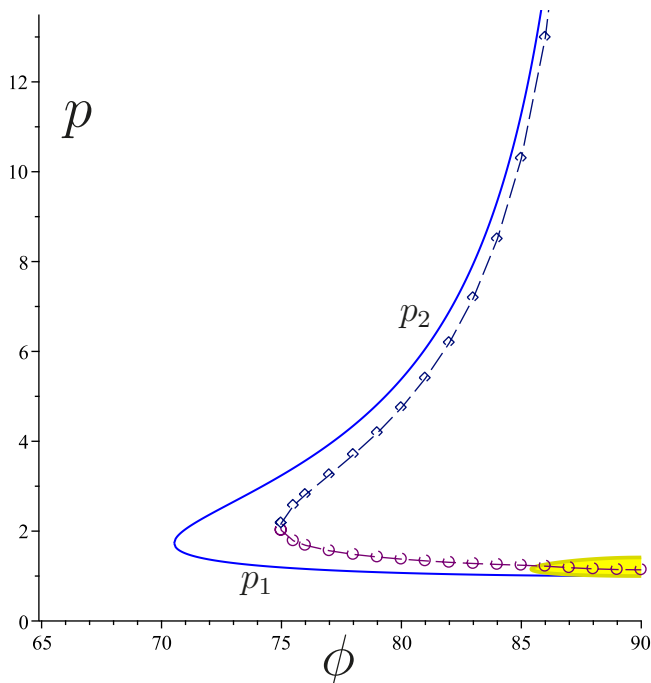


FIG. 7. The solid C-shaped curve represents the asymptotic values p_1 and p_2 given by (25) versus the angle ϕ . The domain colored in yellow represents the region where $\alpha_4 < 0$. The long-wave instability is predicted by the KS equation (20) to occur in $l > 0$ mixtures for values of ϕ and p lying to the right of the solid C-shaped curve excluding the yellow region. In fact, the actual region of this instability in $l > 0$ mixtures is to the right of the dashed C-shaped curve excluding the yellow region. The dashed C-shaped curve is computed by accounting for all roots of the dispersion relation, rather than the root leading to Eq. (20).

occurrence for $Le > 1$. The simulations are based on the numerical solution of the time-dependent problem (1) for finite value of β , $\beta = 10$, in contrast to the theoretical analysis above based on the asymptotic limit $\beta \rightarrow \infty$. As auxiliary conditions, we adopt periodic conditions in the y direction and an initial condition corresponding to a steady, planar premixed flame solution, which is also determined numerically. The computations are carried out using COMSOL MULTIPHYSICS software as described in [2,7]. The domain sizes in the x and y directions are chosen to be $40\sqrt{1 + p^2 c^2}$ and $100\sqrt{1 + p^2 s^2}$, respectively. A nonuniform grid with typically 300 000 triangular elements is chosen with local refinement around the reaction zone. A technical aspect to point out is that although U in Eqs. (1) corresponds to the propagation speed of the unperturbed planar flame which is time independent, it is considered in the computations as a time-dependent unknown parameter. This parameter is determined at each time step so that the flame front remains inside the computational domain. Specifically, U is chosen to be the instantaneous total burning rate per unit transverse flame area U_T given by

$$U_T = \frac{1}{L_y} \iint \omega \, dx \, dy, \quad (27)$$

where L_y is the domain extent in the y direction.

Two values of the Lewis number Le are considered in the simulations, namely, $Le = 0.7$ in Fig. 8 and $Le = 1.6$ in Fig. 9. Plotted in these figures are reaction rate fields at selected times. The left panel in Fig. 8 provides a typical reference case illustrating the evolution of an initially planar flame due to the cellular diffusive-thermal instability in the absence of Taylor dispersion, $p = 0$.

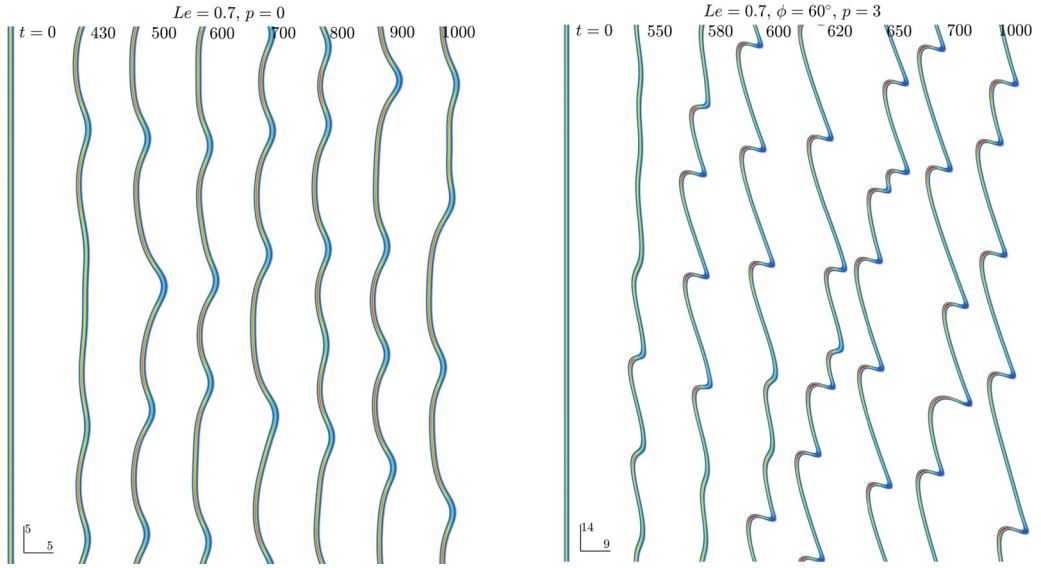


FIG. 8. Reaction rate fields ω at selected times t for $Le = 0.7$, with $p = 0$ (left) and with $p = 3$ and $\phi = 60^\circ$ (right). In all computations, the values $\beta = 10$ and $\alpha_h = 0.85$ are adopted, and the scales for the horizontal x axis and vertical y axis are given in the bottom left corner of each panel.

The flame is seen to evolve into a cellular, apparently chaotic structure, as will be confirmed in Fig. 10 by the plot of its corresponding instantaneous burning speed U_T given by (27). Note in this case that the front of the two-dimensional flame, which may be identified by the location of its thin reaction zone, is characterized by (local) leading edges (parts most protruding towards the unburnt gas, called tips in [23]) which are almost flat and separated by somewhat cusped parts pointing

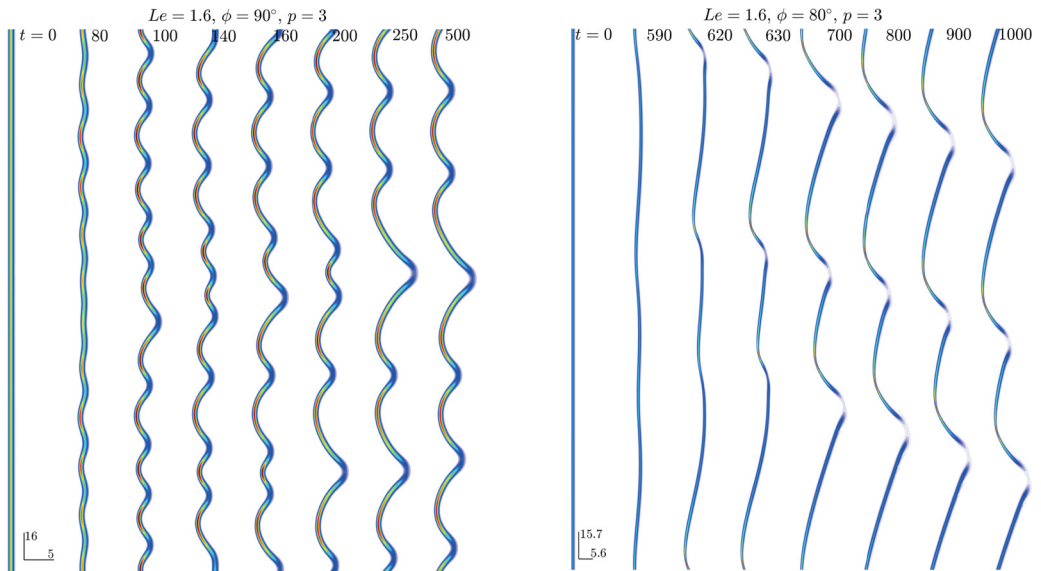


FIG. 9. Reaction rate fields ω at selected times t for $Le = 1.6$ and $p = 3$ with $\phi = 90^\circ$ (left) and $\phi = 80^\circ$ (right).

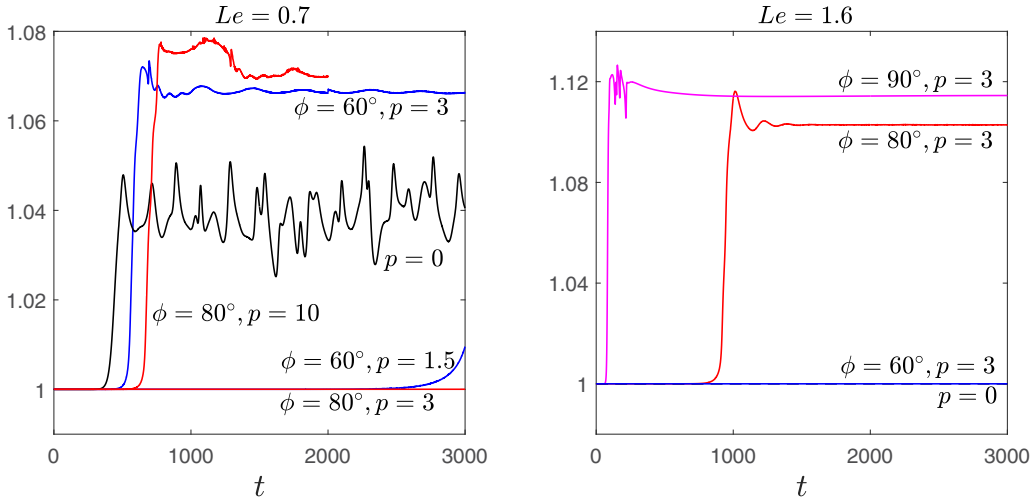


FIG. 10. Effective burning speed U_T [computed according to (27)] versus time t for selected values of Le , ϕ , and p .

towards the burnt gas, as found in the literature [23]. We turn now to the right panel in Fig. 10, which illustrates the influence of Taylor dispersion on the instability of the planar flame when it is oblique to the direction of the shear flow with $\phi = 60^\circ$. A noticeable difference from the left panel is that the leading edges are now sharply curved and have normal vectors which are not aligned with the x direction. Furthermore, there is a clear convective motion in the y direction. For large times, the flame evolves into an apparently steadily propagating structure, as will be confirmed in Fig. 10.

We now examine the $Le = 1.6$ cases presented in Fig. 9. The left panel pertains to $\phi = 90^\circ$ (characterizing a flame initially aligned with the direction of the shear) and $p = 3$. The most noticeable feature of the figure is the demonstration that a cellular instability appears in this case for a Lewis number larger than unity. This is attributable to the fact that the effective Lewis number in the y direction, which is the direction transverse to that of flame propagation, is less than unity in this case. Indeed, the formulas for the effective Lewis numbers Le_x and Le_y given in Eq. (2) imply that $Le_x = 1.6$ and $Le_y = 0.67$, using $s = \sin 90^\circ = 1$, $c = \cos 90^\circ = 0$, and $p = 3$. The fact that it is the Lewis number in the transverse direction, Le_y , which is mainly responsible for the cellular diffusive-thermal instability is not surprising. Indeed, it is well known in the literature that the cellular instability is primarily controlled by the relative magnitude of the heat and mass fluxes transverse to the direction of flame propagation, that is, by Le_y in our case. This point is well explained for conventional flames, e.g., in [24] (see in particular Fig. 4.13 therein) and on pp. 78–79 in [9] (see in particular Fig. 2.8 therein).

Apart from the noticeable occurrence of the instability for $Le > 1$, the flame evolution is largely similar to classical subunity Lewis number cases. We turn to the right panel of Fig. 9 pertaining to $\phi = 80^\circ$. Here the cellular instability also occurs, with the flame having leading edges less flat and with an accompanying net motion in the y direction.

To close this section, we turn to Fig. 10, where the burning speed U_T defined in (27) is plotted versus time. The left panel pertains to $Le = 0.7$. The panel shows that the flame is unstable irrespective of the values of p when $\phi = 60^\circ$. On the other hand, when $\phi = 80^\circ$, the flame is stable for $p = 3$, but unstable for $p = 0$ and 10. This indicates stability for moderately large values of p and instability for smaller and larger values, in agreement with the theoretical predictions represented in Figs. 2 and 6 corresponding to $\phi = 80^\circ$. As for the right panel, pertaining to $Le = 1.6$, it shows that the flame is stable irrespective of ϕ when $p = 0$, as expected. When $p = 3$, the panel also shows that the flame is stable when $\phi = 60^\circ$ and unstable when $\phi = 80^\circ$ and 90° . This emphasizes the

importance of the role played by the direction of flame propagation relative to the direction of the shear, when analyzing flame stability.

VIII. CONCLUSION

We have investigated the diffusional-thermal instabilities of premixed flames, within a two-dimensional constant density model accounting for the effect of Taylor dispersion. The two-dimensional model is obtained upon depth averaging of the three-dimensional governing equations in a configuration resembling that of a Hele-Shaw cell but comprising a shear flow. A linear stability analysis has been carried out to determine the growth rate of perturbations, in terms of the reduced Lewis number l [$l = \beta(\text{Le} - 1)$], the dispersion coefficient p ($p \propto \text{Pe}$), and the angle ϕ between the direction of flame propagation and the direction of the flow. Stability diagrams characterizing the flame instabilities have been determined in terms of these parameters.

One of the key conclusions obtained is the occurrence of cellular instabilities in $\text{Le} > 1$ mixtures if the Péclet number Pe is above a critical value and the angle $\phi \gtrsim 75^\circ$. In general, it is found that an increase in ϕ from 0° to 90° has a stabilizing effect when $\text{Le} < 1$ and a destabilizing effect when $\text{Le} > 1$. The analysis includes the derivation of a modified Kuramoto-Sivashinsky equation describing the onset of a long-wave cellular instability, for any angle ϕ of flame propagation. The equation is found to include a drift term (a first-order spatial derivative) and a dispersion term (a third-order spatial derivative) whenever $\phi \neq 0^\circ$ and $\phi \neq 90^\circ$. The study, which is primarily analytical, is complemented by two-dimensional time-dependent numerical simulations. These are based on the depth-averaged governing equations and performed for selected values of the parameters to support and extend the theoretical findings.

There are no experimental studies in the literature which explore the effect of Taylor dispersion and shear-flow direction on the flame instabilities, including the diffusive-thermal instabilities addressed herein. It would be highly desirable if such studies could be undertaken, to confirm, e.g., our prediction that a cellular instability induced by Taylor dispersion can arise for large Lewis numbers and flames nearly aligned with the direction of the shear, $\phi \gtrsim 75^\circ$.

ACKNOWLEDGMENT

This research was supported by the UK EPSRC through Grant No. EP/V004840/1.

APPENDIX A: JUSTIFICATION OF THE JUMP CONDITIONS

The main aim of this Appendix is to justify jump conditions (10) accounting for anisotropic diffusion. To this end, we first note that these follow from the more general, coordinate-free, form

$$[[\theta^0]] = 0, \quad [[h]] = 0, \quad (\text{A1a})$$

$$[[h_n]] + \frac{1 - p^2(\mathbf{n} \cdot \mathbf{i}_s)^2}{1 + p^2(\mathbf{n} \cdot \mathbf{i}_s)^2} l [[\theta_n^0]] = 0, \quad (\text{A1b})$$

$$[1 + p^2(\mathbf{n} \cdot \mathbf{i}_s)^2]^{1/2} [[\theta_n^0]] = -\exp\left(\frac{h}{2}\right), \quad (\text{A1c})$$

applicable at the reaction sheet located at $n = 0$. Here \mathbf{i}_s is a unit vector in the direction of the shear flow, \mathbf{n} a unit vector normal to the reaction sheet pointing towards the burnt gas, and n a coordinate in the direction of \mathbf{n} . The subscript n represents the partial derivative $\partial/\partial n = \mathbf{n} \cdot \nabla$ and the notation $[[\psi]] = \psi(n = 0^+) - \psi(n = 0^-)$ is used.

The fact that jump conditions (10) follow from (A1) can be checked by noting, with reference to Fig. 1, that $\mathbf{i}_s = c\mathbf{i} - s\mathbf{j}$ (where $c = \cos \phi$ and $s = \sin \phi$) and that the reaction sheet at $x = f(y, t)$ has unit normal vector $\mathbf{n} = (\mathbf{i} - f_y \mathbf{j})/(1 + f_y^2)^{1/2}$ and unit tangential vector $\boldsymbol{\tau} = (f_y \mathbf{i} + \mathbf{j})/(1 + f_y^2)^{1/2}$.

This implies that

$$\frac{\partial}{\partial n} = \mathbf{n} \cdot \nabla = \frac{\partial_x - f_y \partial_y}{(1 + f_y^2)^{1/2}} = (1 + f_y^2)^{1/2} \frac{\partial}{\partial x} - f_y \frac{\partial}{\partial \tau},$$

where $\partial/\partial \tau = \boldsymbol{\tau} \cdot \nabla = (f_y \partial_x + \partial_y)/(1 + f_y^2)^{1/2}$ denotes differentiation in the tangential direction. The expression for $\partial/\partial n$ implies, for any quantity ψ such as θ^0 or h which is continuous across the reaction sheet, i.e., satisfying $[[\psi]] = 0$ and hence $[[\partial\psi/\partial\tau]] = \partial[[\psi]]/\partial\tau = 0$, that

$$\frac{\partial\psi}{\partial n} = (1 + f_y^2)^{1/2} \frac{\partial\psi}{\partial x}. \quad (\text{A2})$$

Using (A2) along with the relation

$$(\mathbf{n} \cdot \mathbf{i}_s)^2 = \frac{(c + s f_y)^2}{1 + f_y^2} \quad (\text{A3})$$

in (A1) leads readily to jump conditions (10).

It remains to justify the coordinate-free form (A1) of the jump conditions. This form follows in fact from the jump conditions fully derived in [1] in the particular case corresponding to $\phi = 0$ in Fig. 1 for which the x direction is chosen to coincide with the direction of the shear, $\mathbf{i} = \mathbf{i}_s$. In this particular case and using the notation of the present paper, it is found that

$$[[\theta^0]] = 0, \quad [[h]] = 0, \quad (\text{A4})$$

$$[[h_x]] + \frac{1 + f_y^2 - p^2}{1 + f_y^2 + p^2} l [[\theta_x^0]] = 0, \quad (\text{A5})$$

$$\sqrt{1 + f_y^2 + p^2} [[\theta_x^0]] = -\exp\left(\frac{h}{2}\right), \quad (\text{A6})$$

applicable at $x = f(y, t)$. Equation (A2) is still applicable in this case, $\phi = 0$, and so is Eq. (A3) with $c = 1$ and $s = 0$, which implies that $1 + f_y^2 = 1/(\mathbf{n} \cdot \mathbf{i}_s)^2$. These two equations allow us to replace in (A5) and (A6) partial derivatives with respect to x with partial derivatives with respect to n and to eliminate f_y , which leads in a straightforward manner to the coordinate-free form (A1), as required.

Using the jump conditions (A1), it is easy to show that the burning speed of a planar flame propagating in the direction of the unit vector \mathbf{n} is given by

$$S_L(\mathbf{n}) = [1 + p^2(\mathbf{n} \cdot \mathbf{i}_s)^2]^{1/2} \quad (\text{A7})$$

in the equidiffusional flame approximation $\beta(\text{Le} - 1) \sim 1$ as $\beta \rightarrow \infty$. For arbitrary Lewis number, this can be generalized to

$$S_L(\mathbf{n}) = \frac{1 + p^2(\mathbf{n} \cdot \mathbf{i}_s)^2}{[1 + p^2(\mathbf{n} \cdot \mathbf{i}_s)^2 \text{Le}^2]^{1/2}}. \quad (\text{A8})$$

In fact, the formulas (A7) and (A8) are equivalent to the formulas (12) and (5) derived in this paper (with $U = S_L$).

For reference, we note that the kinematics of a quasiplanar flame with local burning speed $S_L(\mathbf{n})$ in a fluid with local velocity \mathbf{v} is governed by

$$(\mathbf{v}_{\text{flame}} - \mathbf{v}) \cdot \mathbf{n} = -S_L(\mathbf{n}) \quad (\text{A9})$$

if $\mathbf{v}_{\text{flame}}$ is the flame velocity and \mathbf{n} is chosen to point towards the burnt gas. Thus, if the flame front is described by the relation $F(\mathbf{x}, t) = 0$, then flame propagation is described by the eikonal equation

$$F_t + \mathbf{v} \cdot \nabla F = S_L(\mathbf{n}) |\nabla F| \quad (\text{A10})$$

which follows from (A9) by noting that for points $\mathbf{x}(t)$ on the flame, we have $F_t dt + d\mathbf{x} \cdot \nabla F = 0$ and hence $F_t + (d\mathbf{x}/dt) \cdot \mathbf{n} |\nabla F| = 0$ with $\mathbf{v}_{\text{flame}} \cdot \mathbf{n} \equiv (d\mathbf{x}/dt) \cdot \mathbf{n}$.

APPENDIX B: DERIVATION OF THE DISPERSION RELATION

In this Appendix we provide a derivation of the dispersion relation (15). The methodology used is rather classical (see, e.g., [8]). We begin by substituting the perturbed solutions (13) into Eqs. (6)–(10). This leads to an eigen-boundary-value problem for the functions $\hat{\theta}(x)$ and $\hat{h}(x)$, which is given by

$$(1 + p^2 c^2) \hat{\theta}'' - (U + 2ikp^2 cs) \hat{\theta}' - [\sigma + (1 + p^2 s^2) k^2] \hat{\theta} = 0, \quad (\text{B1})$$

$$\begin{aligned} (1 + p^2 c^2) \hat{h}'' - (U + 2ikp^2 cs) \hat{h}' - [\sigma + (1 + p^2 s^2) k^2] \hat{h} \\ = -l[(1 - p^2 c^2) \hat{\theta}'' + 2ikp^2 cs \hat{\theta}' - (1 - p^2 s^2) k^2 \hat{\theta}] \end{aligned} \quad (\text{B2})$$

for $x \neq 0$, subject to the boundary conditions

$$\hat{\theta} = 0, \quad \hat{h} = 0 \quad \text{as } x \rightarrow \pm\infty \quad (\text{B3})$$

and the jump conditions

$$\llbracket \hat{\theta} \rrbracket = \frac{\hat{f}}{U}, \quad \llbracket \hat{h} \rrbracket = -\frac{l(1 - p^2 c^2) \hat{f}}{U^3}, \quad (\text{B4})$$

$$\llbracket \hat{h}' \rrbracket + \frac{l(1 - p^2 c^2)}{U^2} \llbracket \hat{\theta}' \rrbracket = -\frac{l(1 - p^2 c^2) \hat{f}}{U^4} - \frac{4iklp^2 cs \hat{f}}{U^5}, \quad (\text{B5})$$

$$\llbracket \hat{\theta}' \rrbracket = -\frac{\hat{h}(0^+)}{2U} + \left(\frac{1}{U^2} + \frac{ikp^2 cs}{U^3} \right) \hat{f} \quad (\text{B6})$$

at $x = 0$. We note that the jump conditions (10) at the reaction sheet $x = f(y, t)$ have been transferred to $x = 0$, using Taylor expansions for small values of δ , since $f = O(\delta)$ according to (13).

The solution of the linear differential equations (B1) and (B2) subject to all conditions except (B5) is

$$\hat{\theta} = -\frac{\hat{f}}{U} \begin{cases} e^{r^+ x} \\ 0, \end{cases} \quad \hat{h} = \frac{\hat{f}}{U} \times \begin{cases} [1 - \Gamma + \frac{l}{U^2}(1 - p^2 c^2) + l\chi x] e^{r^+ x} & \text{for } x < 0 \\ (1 - \Gamma) e^{r^- x} & \text{for } x > 0, \end{cases}$$

where

$$r^\pm = \frac{1}{2U} (1 + g' \pm \Gamma),$$

with $g' = \frac{2ikp^2 cs}{U}$, $\Gamma = \sqrt{(1 + g')^2 + 4\sigma + 4k^2(1 + p^2 s^2)}$, and

$$\begin{aligned} \chi &= \frac{1}{U\Gamma} [(1 - p^2 c^2) r^{+2} + 2ikp^2 cs r^+ - (1 - p^2 s^2) k^2] \\ &= \frac{1}{U\Gamma} \left(\frac{1 - p^2 c^2}{4U^2} (1 + g' + \Gamma)^2 + \frac{g'}{2} (1 + g' + \Gamma) - (1 - p^2 s^2) k^2 \right). \end{aligned}$$

In deriving the solution above, unstable modes characterized by $\text{Re}(\sigma) \geq 0$ are assumed, which implies that $\text{Re}(\Gamma) \geq 1$ and hence $\text{Re}(r^+) \geq 0$ and $\text{Re}(r^-) \leq 0$. Applying the condition (B5) to this solution leads, after a few algebraic manipulations, to the dispersion relation

$$2\Gamma^2(\Gamma - 1) + \frac{l}{1 + p^2 c^2} [(\Gamma - 1 - g')(1 - p^2 c^2 + 2g') - 2\sigma(1 - p^2 c^2) + 4k^2 p^2 (c^2 - s^2)] = 0.$$

It is convenient to introduce, as in (14), the variables

$$\tilde{\sigma} = \sigma + ig\tilde{k}, \quad \tilde{k}^2 = k^2 \frac{1+p^2}{1+p^2c^2}, \quad g = \frac{p^2cs}{\sqrt{1+p^2}}$$

in terms of which the dispersion relation takes the form of the dispersion relation (15).

-
- [1] J. Daou, Effect of Taylor dispersion on the thermo-diffusive instabilities of flames in a Hele–Shaw burner, *Combust. Theory Model.* **25**, 765 (2021).
- [2] J. Daou, A. Kelly, and J. Landel, Flame stability under flow-induced anisotropic diffusion and heat loss, *Combust. Flame* **248**, 112588 (2023).
- [3] J. Daou and P. Rajamanickam, Diffusive-thermal instabilities of a planar premixed flame aligned with a shear flow, *Combust. Theory Model.* **1** (2023).
- [4] P. Rajamanickam, A. Kelly, and J. Daou, Stability of diffusion flames under shear flow: Taylor dispersion and the formation of flame streets, *Combust. Flame* **257**, 113003 (2023).
- [5] P. Pearce and J. Daou, Taylor dispersion and thermal expansion effects on flame propagation in a narrow channel, *J. Fluid Mech.* **754**, 161 (2014).
- [6] J. Daou, P. Pearce, and F. Al-Malki, Taylor dispersion in premixed combustion: Questions from turbulent combustion answered for laminar flames, *Phys. Rev. Fluids* **3**, 023201 (2018).
- [7] P. Rajamanickam and J. Daou, A thick reaction zone model for premixed flames in two-dimensional channels, *Combust. Theory Model.* **27**, 487 (2023).
- [8] G. I. Sivashinsky, Nonlinear analysis of hydrodynamic instability in laminar flames—I. Derivation of basic equations, *Acta Astronaut.* **4**, 1177 (1977).
- [9] P. Clavin and G. Searby, *Combustion Waves and Fronts in Flows: Flames, Shocks, Detonations, Ablation Fronts and Explosion of Stars* (Cambridge University Press, Cambridge, 2016).
- [10] G. Joulin and G. Sivashinsky, Influence of momentum and heat losses on the large-scale stability of quasi-2D premixed flames, *Combust. Sci. Technol.* **98**, 11 (1994).
- [11] D. Fernández-Galisteo, V. N. Kurdyumov, and P. D. Ronney, Analysis of premixed flame propagation between two closely-spaced parallel plates, *Combust. Flame* **190**, 133 (2018).
- [12] E. Al Sarraf, C. Almarcha, J. Quinard, B. Radisson, B. Denet, and P. Garcia-Ybarra, Darrieus–Landau instability and Markstein numbers of premixed flames in a Hele-Shaw cell, *Proc. Combust. Inst.* **37**, 1783 (2019).
- [13] F. Veiga-López, M. Kuznetsov, D. Martínez-Ruiz, E. Fernández-Tarrazo, J. Grune, and M. Sánchez-Sanz, Unexpected propagation of ultra-lean hydrogen flames in narrow gaps, *Phys. Rev. Lett.* **124**, 174501 (2020).
- [14] D. Martínez-Ruiz, F. Veiga-López, D. Fernández-Galisteo, V. N. Kurdyumov, and M. Sánchez-Sanz, The role of conductive heat losses on the formation of isolated flame cells in Hele-Shaw chambers, *Combust. Flame* **209**, 187 (2019).
- [15] G. Gu, J. Huang, W. Han, and C. Wang, Propagation of hydrogen–oxygen flames in Hele-Shaw cells, *Int. J. Hydrog. Energy* **46**, 12009 (2021).
- [16] A. Domínguez-González, D. Martínez-Ruiz, and M. Sánchez-Sanz, Stable circular and double-cell lean hydrogen–air premixed flames in quasi two-dimensional channels, *Proc. Combust. Inst.* **39**, 1731 (2023).
- [17] M. C. Cross and P. C. Hohenberg, Pattern formation outside of equilibrium, *Rev. Mod. Phys.* **65**, 851 (1993).
- [18] M. Cross and H. Greenside, *Pattern Formation and Dynamics in Nonequilibrium Systems* (Cambridge University Press, Cambridge, 2009), pp. 75–81.
- [19] G. I. Sivashinsky, Instabilities, pattern formation, and turbulence in flames, *Annu. Rev. Fluid Mech.* **15**, 179 (1983).

- [20] R. J. Tomlin, A. Kalogirou, and D. T. Papageorgiou, Nonlinear dynamics of a dispersive anisotropic Kuramoto–Sivashinsky equation in two space dimensions, *Proc. R. Soc. A* **474**, 20170687 (2018).
- [21] H.-C. Chang, E. A. Demekhin, and D. I. Kopelevich, Laminarizing effects of dispersion in an active-dissipative nonlinear medium, *Physica D* **63**, 299 (1993).
- [22] G. Akrivis, D. T. Papageorgiou, and Y.-S. Smyrlis, Computational study of the dispersively modified Kuramoto–Sivashinsky equation, *SIAM J. Sci. Comput.* **34**, A792 (2012).
- [23] B. Denet and P. Haldenwang, Numerical study of thermal-diffusive instability of premixed flames, *Combust. Sci. Technol.* **86**, 199 (1992).
- [24] G. Joulin and P. Vidal, in *Hydrodynamics and Nonlinear Instabilities*, edited by C. Godrèche and P. Manneville (Cambridge University Press, Cambridge, 1998), p. 536.